Наносистеми, наноматеріали, нанотехнології
Nanosistemi, Nanomateriali, Nanotehnologii
2026, т. 24, № 1, сс. 17–31
https://doi.org/10.15407/nnn.24.01.0017

PACS numbers: 03.65.Ta, 03.65.Yz, 03.67.-a, 03.67.Lx, 73.21.La, 85.25.Am, 85.35.Be

Quantum Fisher Information Tensor and Diagnostic Metrics for Qubit Architectures: Towards Informational Nanotechnologies at the Nanoscale

G. P. Chuiko, Y. S. Darnapuk, and P. K. Kravchenko

Petro Mohyla Black Sea National University,
10, 68-Desantnykiv Str.,
UA-54009 Mykolaiv, Ukraine

Quantum computing is increasingly regarded as a part of information nanotechnology, where reliable diagnostics under realistic noise conditions are crucial. Depolarization channels are commonly used as a fundamental model of quantum noise, but systematic diagnostic frameworks are still underdeveloped. We introduce a structured approach as to computational methods for depolarization channels, establish formal criteria such as metric reliability, and develop diagnostic maps and quantum Fisher information (QFI) tensors. Symbolic modelling of density matrices under noise allows for the analytical calculation of QFI components, revealing the isotropy and degeneracy of tensors at the critical point of Bloch-sphere collapse. Comparing quantum metrics, including purity, entropy, accuracy, Bloch norm, and Bloch-angle deviation (BAD), uncovers different sensitivities. Notably, purity and entropy reach their extremes with minimal uncertainty, while the Bloch norm and BAD quickly detect orientation loss and the inversion of the Bloch vector. The classification of subcritical Bloch-sphere compression, critical collapse, and supercritical inversion is validated, with BAD serving as an operational boundary marker. Potential applications include reliability testing in quantum processors, decoherence diagnostics in nanoscale devices, and benchmarking quantum gates. In Ukraine, this work is among the first systematic studies of a depolarizing quantum-noise channel, enhancing national expertise in diagnostic tools for quantum nanotechnology.

Квантові обчислення все частіше розглядають як частину інформаційних нанотехнологій, де надійна діягностика в реалістичних умовах шуму є критично важливою. Канали деполяризації зазвичай використовують як фундаментальний модель квантового шуму, але систематичні діягностичні рамки все ще недостатньо розроблено. Ми впроваджуємо структурований підхід щодо обчислювальних методів для каналів деполяризації, встановлюємо формальні критерії, такі як метрична надійність, і розробляємо діягностичні карти та тензори квантової інформації за Фішером (КІФ). Символічне моделювання матриць густини в умовах шуму уможливлює аналітично розраховувати компоненти КІФ, виявляючи ізотропію та виродження тензорів у критичній точці колапсу Блохової сфери. Порівняння квантових метрик, включаючи чистоту, ентропію, точність, Блохову норму та девіяцію Блохового кута (ДБК), виявляє різну чутливість. Примітно, що чистота й ентропія сягають своїх крайнощів з мінімальною невизначеністю, тоді як Блохова норма та ДБК швидко виявляють втрату орієнтації й інверсію Блохового вектора. Класифікацію субкритичного стиснення Блохової сфери, критичного колапсу та надкритичної інверсії підтверджено, причому ДБК служить операційним граничним маркером. Потенційні застосування включають тестування надійности квантових процесорів, діягностику декогеренції в нанорозмірних пристроях і порівняльну аналізу квантових вентилів. Ця робота є одним з перших в Україні систематичних досліджень деполяризувального квантового шумового каналу, що розширює національну експертизу в діягностичних інструментах для квантових нанотехнологій.

Key words: quantum nanotechnology, depolarization channel, quantum Fisher information, Bloch-sphere collapse, diagnostic metrics, Bloch-angle deviation.

Ключові слова: квантова нанотехнологія, канал деполяризації, квантова інформація за Фішером, колапс Блохової сфери, діягностичні метрики, девіяція Блохового кута.

(Received 12 January, 2026)

1. INTRODUCTION

Quantum computing is increasingly seen as a specialized area of information nanotechnology for three main reasons. First, it utilizes qubits, nanoscale devices developed through nanotechnology. Second, qubit behaviour and information processing are governed by quantum physics, including superposition, entanglement, and decoherence. Finally, quantum computing introduces a novel method of processing information at the quantum nanoscale, positioning it as an innovative tool for data management.

The intersection of quantum computing and nanotechnology presents significant potential, as quantum computation depends on nanoscale precision and materials [1]. Nanoscale materials are crucial for advancing quantum technologies, including computation and sensing [2]. Moreover, nanotechnology is essential for the creation and control of qubits, where quantum effects exclusively emerge at the nanoscale [3].

Therefore, quantum computing should no longer be viewed merely as a technology that utilizes quantum phenomena; it should be regarded as informational nanotechnology.

Despite advancements in quantum computing and nanotechnology for qubit design, there is a lack of robust diagnostic frameworks for assessing qubit stability and reliability under realistic noise conditions. It often leaves a gap between theoretical research and practical engineering applications in quantum processors.

Although the depolarization channel is widely recognized as a fundamental model for quantum noise [4], there is a lack of understanding of how to systematically quantify and diagnose quantum information loss at the device level. Current methods do not fully utilize quantum Fisher information and related tensor-based metrics to evaluate the informativeness and robustness of qubit states against environmental disturbances.

The depolarization channel is an essential model of quantum noise that explains how quantum information is lost due to environmental disturbances. In this channel, a quantum state is randomly affected by one of the Pauli operators, leading to increased mixedness and a loss of coherence. Superconducting qubits, with short coherence times and strong environmental coupling, are especially vulnerable to this noise [5–7].

This work addresses this gap by developing a comprehensive, computation-based diagnostic framework that links quantum information theory with engineering practice.

By introducing formal criteria like metric validity and self-boundedness and by automating the creation of diagnostic maps and quantum Fisher information tensors, this research provides new tools for real-time evaluation and optimization of nanoscale quantum architectures.

The authors connect quantum information theory with engineering models and analyse quantum channels affected by depolarizing noise [5, 8]. Key aspects include critical points for orientation loss, criteria for metric usability, and self-boundedness for evaluating quantum states in single-shot measurements.

This study advances quantum diagnostics by providing a framework for nanoscale quantum structures in informational nanotechnology [9, 10].

2. SYMBOLIC MODELLING METHODS

Our approach is based on a fundamental concept in quantum mechanics, namely, the density matrix. The density matrix describes the complete statistical state of a quantum system. It extends the idea of a state vector, allowing us to explain both coherent and incoherent superpositions (*i.e.*, mixed states) arising from uncertainty or environmental factors. This framework enables us to calculate expectation values, entropies, and diagnostic metrics, including quantum Fisher information (QFI), purity, and fidelity [10].

Let the density matrix of a pure state of a qubit be ρ. Then, one can write down the standard expression for the matrix of a noisy state [5]:

$$\rho_n = (1-p)\rho + \frac{p}{3}(X\rho X + Y\rho Y + Z\rho Z). \tag{1}$$

In this context, X, Y, and Z represent the well-known Pauli matrices associated with the corresponding quantum gates, while p indicates the depolarization rate [5]. This demonstrates that there is a $(1-p)$ probability that the qubit state remains unchanged. Conversely, there p is a probability that the qubit experiences an equal mixture of three errors.

If one chooses the initial pure state of a qubit in the form

$$|\psi\rangle = \cos\left(\frac{\theta}{2}\right)^2 |0\rangle + \exp(-i\varphi)\sin\left(\frac{\theta}{2}\right)^2 |1\rangle, \tag{2}$$

where θ, φ are the quantum state angular co-ordinates on the Bloch-sphere surface, then, Eq. (1) is as follows:

$$\rho_n = \begin{pmatrix} \dfrac{1+\lambda\cos(\theta)}{2} & \dfrac{\lambda\sin(\theta)}{2}\exp(i\varphi) \\ \dfrac{\lambda\sin(\theta)}{2}\exp(-i\varphi) & \dfrac{1-\lambda\cos(\theta)}{2} \end{pmatrix}, \tag{3}$$

where $\lambda = 1 - 4p/3$. If one sets $\lambda = 1$ (that is, $p = 0$), then, they get the density matrix ρ for a pure initial state.

A couple of essential nuances must be addressed before proceeding with the analysis.

Second, the admissible range of the Bloch-sphere shrink parameter λ requires clarification. In the standard formulation, one typically defines: Then the Kraus probability parameter range is $p \in [0, 3/4]$.

However, several sources [8–11] extend the range to $\lambda \in [-1/3, 1]$. This broader interval arises naturally when the Kraus parameter is interpreted as a probability ($p \in [0,1]$), and it still preserves the channel's entirely positive, trace-preserving (CPTP) character. The extended range allows one to analyse both the critical point (with the collapse of the Bloch sphere at $p = 3/4$) and the overcritical regime, where the Bloch sphere inverts for the noisy state.

In the following sections, we accept the expanded range [8–11] for λ, as it offers a more symmetric and metrically meaningful framework for quantum metrological diagnostics.

Quantum Fisher Information (QFI) is a key concept in quantum metrology, because it defines the ultimate limit on the accuracy of parameter estimation [10]. Often called a monotonic measure, QFI functions as the quantum equivalent of classical Fisher Information (CFI) [12]. While CFI measures how a statistical probability distribution changes with parameter variations, QFI shows how a quantum state responds to tiny changes in a selected parameter.

The Quantum Fisher Information (QFI) is specifically defined for a quantum state with respect to a particular parameter. It quantifies the sensitivity of that state to changes in the parameter through the geometry of quantum statistical manifolds. In this way, QFI establishes a practical connection between the structure of quantum states and the maximum measurement precision achievable [10].

The calculation of QFI using symmetric logarithmic derivatives (SLDs) is explained in Ref. [12] and clarified further in Ref. [13]. In this study, we adopt the methods described in those sources. While the approaches in Refs. [12] and [13] offer analytical formulas for the components of the QFI metric tensor in simple quantum systems, it is essential to note that 'standard numerical procedures based on eigen decomposition quickly become impractical with increasing system size' [10].

The noisy density matrix (3) depends on three parameters: either (λ, θ, φ) or equivalent (p, θ, φ), with the Kraus probability (p) offering the more straightforward physical interpretation. Consequently, the quantum Fisher information (QFI) metric tensor is defined as a 3×3 matrix

$$\mathbf{F}(p,\theta,\varphi) = \begin{pmatrix} F_{pp} & F_{p\theta} & F_{p\varphi} \\ F_{\theta p} & F_{\theta\theta} & F_{\theta\varphi} \\ F_{\varphi p} & F_{\kappa\theta} & F_{\varphi\varphi} \end{pmatrix}. \tag{4}$$

Similarly, any quantum metric (m) derived from the density matrix can be expressed as a function $m(p, \theta, \varphi)$.

The quantum Cramér–Rao bound (QCRB) establishes the minimal achievable variance of an unbiased estimator for a single-shot measurement and is a cornerstone of quantum metrology [14, 15]. For a scalar metric observable, the bound is expressed in terms of the gradient and the inverse of the QFI matrix:

$$\Delta_m = \nabla m(p,\theta,\varphi)^\dagger \cdot \mathbf{F}^{-1}(p,\theta,\varphi) \cdot \nabla m(p,\theta,\varphi)\,. \tag{5}$$

The QFI matrix defines the geometry of the quantum statistical manifold, while the gradient maps the metric's dependence on this geometry. In turn, quadratic form (5) provides the tightest lower bound on the variance of the single-shot estimation for the metric.

Let us consider the Bloch vector of a noisy state, for example,

$$\mathbf{b}_n = \begin{pmatrix} Tr(\rho_n X) \\ Tr(\rho_n Y) \\ Tr(\rho_n Z) \end{pmatrix} = \begin{pmatrix} \lambda \sin(\theta)\cos(\varphi) \\ -\lambda \sin(\theta)\sin(\varphi) \\ \lambda \cos(\theta) \end{pmatrix}. \quad (6)$$

The Euclidean norm of this vector, which is clearly equal to the absolute value of λ, can serve as a scalar measure that depends solely on the Kraus parameter, since λ is defined as $(1 - 4p/3)$. This scalar captures the isotropic compression of the Bloch sphere caused by the depolarizing noise channel. At the critical point ($p = 3/4$ and $\lambda = 0$), the Bloch vector completely collapses, and for $\lambda < 0$, it inverts, marking the transition into the overcritical regime.

Additionally, one can calculate the variance (or its square root, called uncertainty) of this measure, if the quantum Fisher information tensor (QFI) is known. This is especially relevant for p-intervals, where the uncertainty of a single test does not surpass the metric. As a result, repeated measurements are unnecessary, saving resources, particularly, time, which is often the most valuable.

3. RESULTS AND DISCUSSION

Let the indices α and β range over all pairs from the set of parameters (p, θ, φ). Then, the elements of the QFI metric tensor (**F**) can be expressed as follows:

$$F_{\alpha\beta} = \left(\frac{1}{2}\right) Tr\left(\rho_n \left\{L_\alpha, L_\beta\right\}\right). \quad (7)$$

Here, $\left\{L_\alpha, L_\beta\right\}$ is the anticommutator of the two SLD matrices mentioned above. The following matrix equation defines them [14, 15]:

$$\frac{\partial \rho_n}{\partial x_\alpha} = \left(\frac{1}{2}\right)\left\{\rho_n, L_\alpha\right\}\left(x_\alpha \in (p, \theta, \varphi)\right). \quad (8)$$

The main computational challenge arises from the fact that the dimensions of all matrices in the system grow exponentially as 2^n, where n is the number of qubits [15]. However, for a single qubit ($n = 1$), there are no significant issues, and the analytic forms of the three operators $\mathbf{L}_\alpha$ are provided in Table 1.

Considering these and the expression (7), $\mathbf{F}(p, \theta, \varphi)$ can be uttered in the following form:

TABLE 1. Analytic expressions for symmetrical logarithmic derivatives (SLDs).

Parameter	$\mathbf{L}_\alpha$
Kraus parameter, p	$\frac{3}{4p(p-3/2)}\begin{pmatrix} \cos(\theta)-1+4p/3 & \sin(\theta)\exp(i\varphi) \\ \sin(\theta)\exp(-i\varphi) & -\cos(\theta)-1+4p/3 \end{pmatrix}$
Polar angle, θ	$(4p/3-1)\begin{pmatrix} \sin(\theta) & -\cos(\theta)\exp(i\varphi) \\ -\cos(\theta)\exp(-i\varphi) & -\sin(\theta) \end{pmatrix}$
Azimuthal angle, φ	$(4p/3-1)\sin(\theta)\begin{pmatrix} 0 & -\exp(i\varphi) \\ \exp(-i\varphi) & 0 \end{pmatrix}$

$$\mathbf{F} = \begin{pmatrix} \frac{2}{p(3-2p)} & 0 & 0 \\ 0 & (1-4p/3)^2 & 0 \\ 0 & 0 & (1-4p/3)^2\sin(\theta)^2 \end{pmatrix}. \tag{9}$$

A diagonality in the QFI (Quantum Fisher Information) metric tensor shows that the parameters (p, θ, φ) are statistically independent directions in quantum information geometry. Since there are no cross-terms (covariances) between these parameters, their sensitivities to changes can be measured separately. In other words, estimating p does not affect the analysis of θ or φ, and *vice versa*.

QFI metric tensor is invertible almost everywhere, excepting the critical point $p = 3/4$. It means that the quantum Cramér–Rao bound (QCRB; see expression (5)) is well defined. Thus, the tensor provides a valid Riemannian metric on the parameter space; so, the geometry is non-degenerate.

At $p = 3/4$, the Bloch sphere collapses to a single point ($\mathbf{b}_n = \mathbf{0}$). The angular part of the QFI tensor (related to θ and φ) becomes degenerate because angles lose meaning, when the Bloch-vector length drops to zero. However, the radial component (the p-direction) remains well defined, so estimating the noise strength is still feasible. Physically, this means that, once the state is maximally mixed, one cannot extract orientation information, *i.e.*, the system carries no angular information.

This interesting observation was previously noted in Refs. [16, 17]. They highlighted that the channel's spherical symmetry causes all angular information to disappear once the Bloch sphere shrinks to the maximally mixed state. As a result, the QFI tensor becomes degenerate in its angular block at the critical point. At the same

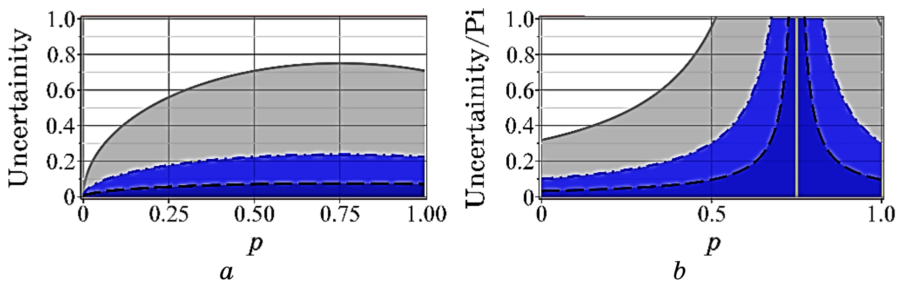

Fig. 1. Displaying the uncertainties (standard deviations) for two parameters: *a*) the Kraus parameter (p), which represents the noise strength, and *b*) the polar angle (θ), which defines the quantum-state position on the Bloch sphere (these uncertainties are normalized to π). The top edges of the shaded regions depict the uncertainties as functions of p across different scenarios: at a single-shot trial ($N = 1$; grey solid line); after $N = 10$ measurements (dark dash-dot line); after $N = 100$ measurements (dashed line).

time, the radial component related to the noise strength stays finite and can still be estimated.

The diagonality and invertibility of the QFI metric tensor (9) indicate that the depolarizing channel maintains isotropy, meaning the informational geometry is separable. At the critical point, only angular information is lost, while scalar metrics depending solely on the Kraus parameter p remains unaffected. Even when the Bloch sphere collapses and orientation information cannot be obtained, it is still possible to estimate the noise parameter p.

The uncertainty in the Kraus parameter (p) shows a local maximum of 3/4 at the critical point, indicating that a single estimate near collapse is unreliable. This highlights the need for repeated measurements to ensure accuracy, reflecting the complex interplay between isotropy, tensor degeneracy, and operational sensitivity.

Using Eqs. (5) and (9), we determine the minimum uncertainties for p and θ. Figures 1, *a* and *b* display these uncertainties for both single-shot and repeated measurements as functions of noise strength p. In single-shot scenarios, uncertainties stay significant across most of the p range, making repeated measurements more effective for achieving reasonable precision.

Note that Fig. 1, *b* also shows the minimal uncertainties of the azimuthal angle φ, observed at $\theta = \pi/2$, which is on the equator of the Bloch sphere. The uncertainties of the Kraus parameter vary smoothly, with a local maximum at the critical point ($p = 3/4$). In contrast, the angular uncertainties exhibit a singularity there, reflecting the geometric loss of orientation information at maximal mixing, as mentioned above.

Quantum metrics are mathematical tools used to measure changes in quantum states, especially, the decoherence, caused by noise. The selection of appropriate quantum metrics to describe a specific noise channel, such as depolarizing noise, is not strictly fixed. Instead, it depends on expert judgment influenced by two main factors.

Contextual Relevance. The chosen metric must align with the researcher's physical intuition and the operational goals of the analysis, whether it is tracking coherence loss, estimating parameters, or benchmarking quantum operations.

Channel Behaviour Specificity. Some metrics are selectively sensitive to certain types of noise. For example, purity might be particularly useful for decoherence, while fidelity is often favoured as a measure of quantum gate performance.

Our short list of metrics, which is presented in Table 2 in a bit of detail, of quantum metrics for depolarizing includes several essential measures: the Quantum Fisher Information (QFI) mentioned earlier, purity, the Bloch-vector norm, von Neumann entropy, fidelity, and a less common but specific metric: the angle between pure and noisy Bloch vectors.

In a depolarizing channel, the qubit's action is isotropic, causing uniform contraction of the Bloch sphere by a factor represented by the Kraus parameter, which indicates noise strength. This contrac-

TABLE 2. List of quantum metrics for the depolarizing noise channel.

Metric	Definition	Operational Role	Sensitivity
Quantum Fisher Information (QFI)	Derived from derivatives of the density matrix with respect to parameters (see Eq. (9))	Precision bounds for parameter estimation	Sensitive to parameter changes (*e.g.*, Kraus parameter p)
Purity	$Tr\left(\rho_n^2\right)$	Tracks decoherence strength	Decreases monotonically with noise
Bloch-vector norm	$\lVert \mathbf{b}_n \rVert$	Geometric measure of coherence	Shrinks isotropically under depolarization
von Neumann entropy	$-Tr\left(\rho_n \log_2 \rho_n\right)$	Quantifies disorder and information loss	Increases with mixing
Fidelity	$\left(Tr\sqrt{\sqrt{\rho}\rho_n\sqrt{\rho}}\right)^2$	Benchmarking gate/channel performance	Sensitive to overlap with the target state
Bloch-angle deviation	Angle between pure and noisy Bloch vectors	Diagnosis of angular information collapse	Sensitive to orientation loss and inversion

tion affects scalar metrics such as those in Table 2 making them dependent solely on the noise strength and ignoring angular orientation. In contrast, Quantum Fisher Information (QFI) involves derivatives of the density matrix, making it sensitive to both angular and radial variables. This difference allows QFI to detect directional degeneracies at critical points.

Figure 2 shows the results of calculations for quantum metrics along with their uncertainties, presented as scalar functions of the Kraus parameter. The critical point manifests differently across these metrics: purity and von Neumann entropy show extrema indicating maximum mixing; the Bloch-vector norm exhibits a distinct corner, signalling collapse and reversal of orientation; while fidelity, relative to the input pure state, remains smooth and unaffected by the criticality, as it depends only on overlap and not on orientation. Together, these results highlight the selective sensitivities of scalar metrics some directly capture the collapse of coherence, while others are unaffected by the geometric singularity.

Uncertainties in quantum metrics respond to the critical point in two diverse ways. Fidelity and the Bloch-vector norm show local maxima, indicating instability in single-shot estimation near the

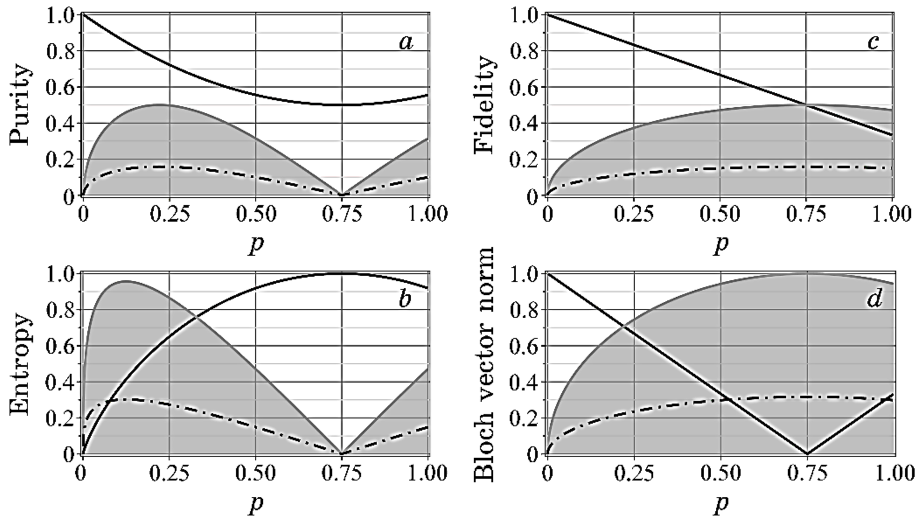

Fig. 2. Presenting various metrics along with their uncertainties (standard deviations) plotted against the Kraus parameter p. The metrics displayed include (a) purity, (b) fidelity, (c) entropy, and (d) Bloch-vector norm. The solid black lines represent the metrics themselves, while the solid gray lines and shaded areas indicate the uncertainties for a single-shot measurement ($N = 1$). Additionally, the dash-dot lines represent the uncertainties after conducting $N = 10$ measurements.

collapse point. In contrast, purity and von Neumann entropy have sharp corners, where uncertainty drops to zero. This dichotomy highlights the operational trade-offs: single-shot trials are feasible for purity, but they remain difficult for the Bloch-vector norm, except in a narrow low-noise regime. Additionally, the extreme values of purity and entropy at the critical point coincide with the minimum uncertainty, suggesting that these metrics can serve as reliable probes for quantum metrology in depolarizing channels. Therefore, the collapse point is not just a singularity in geometry but also a region of improved diagnostic precision for specific scalar measures.

The concept of Bloch-sphere collapse at the dephasing channel's critical point suggests that the norm of the Bloch vector can be measured directly; however, this is impractical. Uncertainty dominates near the crucial point, making it impossible to pinpoint the moment of collapse due to statistical fluctuations. Thus, the zero norm serves as a geometric indicator rather than a measurable quantity. This emphasizes the need to focus on other diagnostics, like purity or entropy, which offer more practical insights into depolarizing dynamics with a less uncertainty at critical points.

The Bloch-angle deviation (BAD) normalized by π exhibits a Heaviside step function dependent on the Kraus parameter p. At the critical point, the Bloch vector collapses, and BAD undergoes a discontinuous jump. Consequently, the derivative of BAD with respect to p is the Dirac delta function: identically zero across the entire domain except at the critical point, where it diverges to infinity. This singular derivative defines the uncertainty of BAD, which remains negligible everywhere except precisely at the collapse.

Operationally, this behaviour indicates that BAD can be measured with nearly zero uncertainty on either side of the critical point, but not precisely at the point itself. In metrological terms, one can 'capture' use brackets around the collapse measurement from both directions a strategy like the artillerymen's phrase 'into a fork', where the target is localized by bounding shots from opposite sides. This property makes BAD a uniquely precise diagnostic: it remains insensitive to criticality yet maximally discriminates between states before and after collapse. In this way, BAD provides a sharp operational boundary marker for the depolarizing channel, complementing scalar metrics that smooth over the transition.

It is worthwhile revisiting the discussion of parameter ranges for the depolarizing channel introduced in Sec. 2. For the Kraus parameterization, the contraction factor takes values, with representative noise strength. Within this framework, the channel exhibits a distinct internal structure.

Subcritical mode ($1 \geq \lambda > 0$ *and* $1 \geq p > 3/4$). The Bloch sphere undergoes isotropic shrinkage and the normalized BAD remains zero, indicating that the orientation of the Bloch vector is preserved.

Critical point ($\lambda = 0$ *and* $p = 3/4$). The Bloch sphere collapses, and BAD becomes undefined. This marks the singular transition between depolarizing and repolarizing behaviour.

Overcritical mode ($0 > \lambda \geq -1/3$ *and* $3/4 < p \leq 1$). The Bloch sphere reverts to its original size, but is flipped in orientation, with BAD set to 1. This flip corresponds to a repolarizing regime, where states are mapped to their antipodes.

The internal structure of the depolarizing noise channel, described here as the taxonomy of subcritical contraction, critical collapse, and overcritical inversion, has been well supported by academic literature for the last two decades. This structure can be divided into three types: subcritical contraction, critical collapse, and overcritical inversion. Early research in Ref. [18] has expanded the Kraus representation of the depolarizing channel to include memory effects, noting that the contraction factor λ can take negative values. This suggests an inversion of the Bloch-vector direction. Such results confirm the existence of an overcritical regime, where the Bloch sphere not only recovers its magnitude, but also reverses its orientation. Pang and co-workers in Ref. [19] experimentally demonstrate that even fully depolarized channels (zero capacity, collapsed Bloch sphere) can regain operational utility. This aligns with our interpretation of the post-collapse regime, in which diagnostic strategies such as BAD bracketing ('taking into account') can extract information despite the collapse.

Recent studies reinforce the distinction between metrics at key points. The authors of Ref. [20] highlight singularities and unstable trajectories in depolarizing maps, indicating that geometric measures, such as the Bloch-vector norm, show significant uncertainty near collapse. Furthermore, Ref. [21] demonstrated that entropy-based diagnostics enter 'absolute regimes' under depolarizing conditions, serving as reliable markers with minimal uncertainty. The paper [22] emphasizes that fidelity is smooth and insensitive to collapse, which aligns with our finding that fidelity does not distinguish between regimes. Burrell extends the geometric analysis of generalized depolarizing channels, confirming that contraction factors crossing zero correspond to an inversion of orientation [23].

4. CONCLUSIONS

In conclusion, the depolarizing channel has a complex internal structure that a single diagnostic cannot fully capture. While traditional measures such as purity, entropy, and fidelity track behaviour across noise regimes, geometric diagnostics like the Bloch-vector norm and BAD more clearly illustrate singular collapse and inversion. To synthesize these findings, Table 3 summarizes the behaviour and uncertainty of each metric across the subcritical, critical, and overcritical regimes, providing the reader with a clear operational map of the channel's diagnostic landscape.

In computer engineering, the taxonomy of depolarizing noise channel regimes and the uncertainty analysis can enhance reliability modelling and error-aware scheduling in quantum processors. This ensures that nanosystems avoid unstable operating points that could lead to collapse. In the realm of informational nanotechnologies, metrics such as purity and entropy, which maintain minimal uncertainty at the critical point, serve as robust indicators for controlling decoherence in nanoscale devices, ranging from spintronic circuits to quantum dots. In quantum computing, BAD can be a precise diagnostic tool for benchmarking channels and gates, comple-

TABLE 3. Comparative synthesis of the behaviour and uncertainty of key quantum metrics across the subcritical, critical, and overcritical regimes of the depolarizing channel.

Metric	Subcritical mode	Critical point	Overcritical mode	Uncertainty behaviour
Purity	Smoothly decreases with p; coherence is gradually lost	Minimum value at the collapse point	Increases with p; symmetric about the critical point	Corner with minimal uncertainty at the collapse point; feasible single-shot estimation
Entropy	Increases with p; mixing grows	Maximum entropy (maximally mixed state)	Decreases with p; symmetric behaviour	Corner with minimal uncertainty at the collapse point; strong metrological probe
Bloch vector norm	Shrinks isotopically	Zero (Bloch sphere collapses to a point)	Continues decreasing; unaffected by inversion	Local maximum in uncertainty; insensitive to collapse but noisy near criticality
Fidelity	Decreases linearly with p	Smooth, no singularity	Continues decreasing; unaffected by inversion	Local maximum in uncertainty; insensitive to collapse but noisy near criticality
BAD (Bloch Angle Deviation)	0 (orientation preserved)	Undefined (collapse)	1 (orientation flipped to antipode)	Zero uncertainty everywhere except a Dirac-delta spike at collapse; measurable 'fork' strategy available

menting fidelity measurements by distinguishing between depolarizing and repolarizing regimes. Additionally, the 'fork' strategy for measuring BAD near the point of collapse suggests new methods for single-shot estimation in quantum metrology. Furthermore, identifying overcritical inversion is linked to recent experimental advances in zero-capacity recovery through channel superposition [19].

These opportunities highlight both the innovative ideas and practical uses of the proposed diagnostic framework. By combining geometric representations, uncertainty analysis, and metrological feasibility, this study lays a foundation for future work in quantum information science and engineering. A clear understanding of qubit behaviour at critical points is crucial for both theoretical and practical progress in these areas.

Despite extensive literature on quantum noise, the authors found limited publications by Ukrainian researchers on depolarizing channels in quantum nanosystems. This does not reflect a lack of interest; active research continues in related fields. Our study aims to be among the first systematic investigations in Ukraine focused on quantum metrology of noise channels, contributing to the global dialogue on quantum information geometry and advancing quantum computing and nanotechnology research in Ukraine.

This study introduces BAD as a new diagnostic tool and presents one of the First systematic uncertainty analyses of scalar and geometric measures of depolarizing noise. While the current research focuses on single-qubit channels, future studies should expand to include multi-qubit systems and incorporate correlated noise to improve applicability. By identifying which metrics remain dependable near the point of collapse, this framework will support the development of robust quantum metrology protocols. Additionally, it will be valuable for fault-tolerant architectures and diagnostic tools essential for scalable quantum nanotechnologies.

REFERENCES

1. M. Nayak and S. K. Moharana, *NanoMind: Exploring Synergies in Nanotechnology and Machine Learning*, **27**: 197 (2025); https://doi.org/10.1007/978-3-031-77296-2_9
2. Q. Dai, C.-Y. Lu, and Z. Sun, *Nanoscale*, **15**, Iss. 26: 10858 (2023); https://doi.org/10.1039/D3NR90099A
3. Talha Nadeem, Tariq Rafique, Waseem Khan, Sahadat Khandakar, Ahmad Alkhayyat, Mahesh Lohith K S, Zemate Achraf Abdelghafour, and Sedra Moulay Brahim, *Nanotechnology Perceptions*, **20**: Iss. 15: 248 (2024). https://doi.org/10.62441/nano-ntp.vi.3463
4. M. Urbanek, B. Nachman, V. R. Pascuzzi, A. He, C. W. Bauer, and W. A. de Jong. *Phys. Rev. Lett.*, **127**, Iss. 27: 270502 (2021); https://doi.org/10.1103/PhysRevLett.127.270502

5. B. Khanal and P. Rivas, *Mathematics*, **12**, Iss. 9: 1385 (2024); https://doi.org/10.3390/math12091385
6. A. Blais, A. L. Grimsmo, S. M. Girvin, and A. Wallraff, *Reviews of Modern Physics*, **93**, Iss. 2: 025005 (2021); https://doi.org/10.1103/RevModPhys.93.025005
7. A. Somoroff, Q. Ficheux, R. A. Mencia, H. Xiong, R. Kuzmin, and V. E. Manucharyan. *Phys. Rev. Lett,* **130**, Iss. 26: 267001 (2023); https://doi.org/10.1103/PhysRevLett.130.267001
8. E. Martinez, A. deMarti iOlius, and P. M. Crespo, *Phys. Rev. A*, **108**, Iss. 3: 032602 (2023); https://doi.org/10.1103/PhysRevA.108.032602
9. S. L. Braunstein and C. M. Caves, *Phys. Rev. Lett*, **72**, Iss. 22: 3439 (1994); https://doi.org/10.1103/PhysRevLett.72.3439
10. G. Wyjtowicz, S. F. Huelga, M. M. Rams, and M. B. Plenio, *Phys. Rev. A*, **112**, Iss. 5: 052410 (2025); https://doi.org/10.1103/xjln-7ddy
11. M. A. Nielsen and I. L. Chuang, *Quantum Computation and Quantum Information: 10th Anniversary Edition* (Cambridge Univ. Press: 2010).
12. P. Denes and C. G. Ghinea, *Quantum Probability and Related Topics. Proceedings of the 30th Conference (23–28 November, 2009)* (Eds. Rolando Rebolledo and Miguel Orszag) (Santiago, Chile: 2011), p. 261–281; https://doi.org/10.1142/9789814338745_0015
13. M. Yu, D. Li, J. Wang, Y. Chu, P. Yang, M. Gong, N. Goldman, and J. Cai, *Phys. Rev. Research*, **3**, Iss. 4: 043122 (2021); https://doi.org/10.1103/PhysRevResearch.3.043122
14. M. Hayashi and Y. Ouyang, *Quantum*, **9**: 1806 (2025); https://doi.org/10.22331/q-2025-07-22-1806
15. J. R. Hervas, A. Z. Goldberg, A. S. Sanz, Z. Hradil, J. Reháček, and L. L. Sánchez-Soto, *Phys. Rev. Lett*, **134**, Iss. 1: 010804 (2025); https://doi.org/10.1103/PhysRevLett.134.010804
16. J. Liu, H. Yuan, X.-M. Lu, and X. Wang, *Journal of Physics A: Mathematical and Theoretical*, **53**: 023001 (2019); https://doi.org/10.1088/1751-8121/ab5d4d
17. F. Albarelli, M. G. Genoni, M. A. C. Rossi, and D. Tomaselli, *Quantum*, **2**: 110 (2018); https://doi.org/10.22331/q-2018-12-03-110
18. S. Daffer, K. Wydkiewicz, J. D. Cresser, and J. K. McIver, *Phys. Rev. A*, **70**, Iss. 1: 010304R (2004); https://doi.org/10.1103/PhysRevA.70.010304
19. A. O. T. Pang, N. Lupu-Gladstein, H. Ferretti, Y. B. Yilmaz, A. Brodutch, and A. M. Steinberg, *Quantum*, **7**: 1125 (2023); https://doi.org/10.22331/q-2023-10-03-1125
20. A. Abu-Nada, S. Banerjee, and A. Sabale, *Phys. Rev. A*, **110**, Iss. 5: 052209 (2024); https://doi.org/10.1103/PhysRevA.110.052209
21. T. Patro, K. Mukherjee, and N. Ganguly, *Quantum Inf. Process.*, **23**: 228 (2024); https://doi.org/10.1007/s11128-024-04439-1
22. B. Khanal and P. Rivas, *Mathematics*, **12**, Iss. 9: 1385 (2024); https://doi.org/10.3390/math12091385
23. C. K. Burrell, *Phys. Rev. A*, **80**, Iss. 4: 042330 (2009); https://doi.org/10.1103/PhysRevA.80.042330